Exp. Theo. NANOTECHNOLOGY 5 (2021) 159 – 169

Experimental and Theoretical NANOTECHNOLOGY
http://etn.siats.co.uk/

Enhancement of low carbon steel corrosion resistance in acidic and saline media using superhydrophobic nanocomposite

Omar A. Abdulrazzaq[1], Siham M. Saeed[2], Zainab H. Ali[2], Saad A. Tuma[1], Omar A. Ahmed[2], Abdulkareem A. Faridoon[2], Shaima K. Abdulridha[1]*

[1]Renewable Energy and Environment Research Center/ Corporation of Research and Industrial Development/ Ministry of Industry and Minerals/ Baghdad-Iraq
[2]Chemical and Petrochemical Research Center/ Corporation of Research and Industrial Development/ Ministry of Industry and Minerals/ Baghdad-Iraq
[*]E-mail: omarsatar2003@gmail.com

Received: 21/2/2020 / *Accepted:* 25/7/2020 / *Published:* 1/5/2021

Superhydrophobic anticorrosion layers of various thicknesses were deposited onto low carbon steel. The layer is comprised of MnO2/Polystyrene nanocomposite with a hierarchical structure. AFM imaging of the nanocomposite illustrated a very rough surface with rms roughness of 109 nm. A polarization method was applied to measure the corrosion potential and corrosion current by using a potentiostat device. Two corrosive solutions were utilized in this study (NaCl & HCl). Strong concentrations of 1M HCl and 5000ppm NaCl were used in this work. The results revealed that the nanocomposite exhibits better corrosion inhibition after 24h immersion time in NaCl compared to HCl, where the corrosion current density is 0.56 µA/cm2 in NaCl against 24.3 µA/cm2 in HCl. The uncoated sample presented a higher corrosion current density after 24h immersion time with values of 14.4 µA/cm2 and 83.6 µA/cm2 in NaCl and HCl, respectively. Moreover, the ultrathin layers of the nanocomposite demonstrated better corrosion inhibition than the relatively thicker layers. This result was elucidated by the peeling effect of the thick samples. Immersion time was also considered in this study by leaving the samples over a course of 30 days in the solution and performing the measurements for every 10 days' span. The activation energy of the surface was determined using Arrhenius method by varying the solution temperature during measurements. Corrosion protection efficiency showed excellent results with up to 96.1% in NaCl solution. Pitting potential was also determined in this work.

Keywords: Superhydrophobic surface; Low carbon steel; Corrosion current.

1. INTRODUCTION

Corrosion of metals in a general sense is a natural process in which metal is gradually destructed in a chemical or electrical media to a more chemically stable form, such as metal oxide. Most metals are very vulnerable to environment and easy to corrode to return back to their stable oxide forms (the ore forms) [1]. Corrosion is a major headache in the industry. The global annual loss due to corrosion is estimated

Exp. Theo. NANOTECHNOLOGY 5 (2021) 159 – 169

to be up to 5% of the economy [2]. Steel (iron alloys) is one of the largest metal industry. However, corrosion takes place in steel more than any other metals. According to NACE International study published in 2016, steel corrosion losses are estimated to be 15% – 35% [3]. Several methods have been used to prevent corrosion, such as cathodic protection, corrosion inhibitors, and protective coatings. The last one is the most commonly used method [4]. The protective coatings have other advantages in addition to corrosion protection over other methods; they improve the wear resistance and could also adorn the surface in some circumstances. Polystyrene is one of the widely used and preferred polymeric protective coatings [5]. However, polymeric coating has some obstacles such as low adhesion and thermal mismatch which can cause peeling off the polymer layer [6]. This problem becomes more manifest when the polymer layer is thick. On the other hand, coating with thin layer is hard to be achieved with pore-free surface. Pores create corrosion sites and reduce the corrosion protection. Another type of protective coatings is the nanostructured coatings. Nanostructures exhibit better corrosion resistance by eliminating the localized corrosion [4]. Nanomaterials can be blended with polymers to form a polymer-based nanocomposite. This composite combines the advantages of polymer and nanomaterials. Superhydrophobic coating is one of these polymer-based nanocomposites.

Superhydrophobicity (so-called lotus effect) is a property of some rough surfaces to repel water. The criterion of this property is the high contact angle (>150°). In rough surfaces, wetting can be classified into homogeneous wetting and heterogeneous wetting [7]. In the first one, the liquid penetrates the grooves of the roughness, while in the latest one, the liquid stays over the summits of the hills leaving a buffer layer of air between the liquid and the surface. This case makes the liquid in the least contact with the surface. The contact angle (θ^*) in heterogeneous wetting is given by Cassie-Baxter equation [8]: $\mathbf{\cos(\theta^*) = r_f \cos(\theta_Y) + f - 1,}$ where θ_Y is the ideal Young contact angle, r_f is the roughness ratio of the solid surface area wetted by the liquid, and f is the fraction of the solid surface area wetted by the liquid. For a repeating pattern of structures, f = (area of top structure)/ (area of repeating lattice). Therefore, for a smooth surface, f = 1, and the Cassie-Baxter model collapses into a trivial solution of Wenzel [$\cos(\theta_W) = r \cos(\theta_Y)$], where θ_W is Wenzel contact angle, and r is the roughness ratio. The wetting regime that gives the lowest contact angle is the more stable topography with high surface energy. Therefore, obtaining a superhydrophobic surface with low surface energy is a matter of sophisticated technology. The superhydrophobic surface has a unique topography so-called "hierarchical structure" which is a set of hills, each one has plenty of protrusions of nanorods. Figure (1) illustrates the hierarchical structure in lotus leaf. This structure can maintain a low surface energy and a high contact angle (usually >150°) which are the main features of superhydrophobicity.

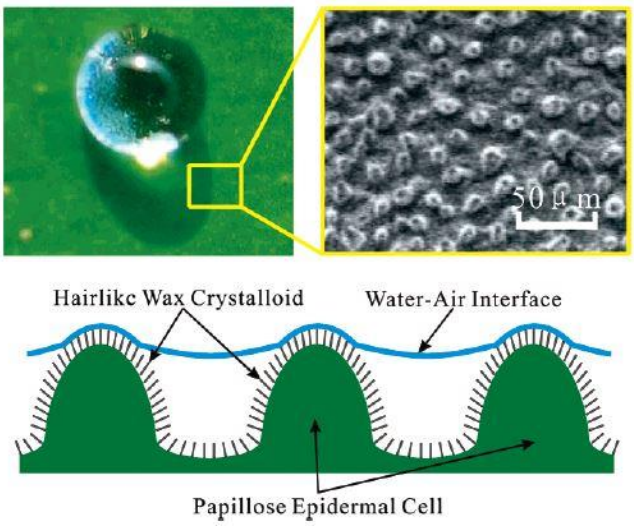

Figure 1 The hierarchical structure of the surface of lotus leaf. *This figure is reproduced from* [9].

Exp. Theo. NANOTECHNOLOGY 5 (2021) 159 – 169

Superhydrophobic coatings have received an increasing attention in recent years because of their high water repellency. This unique feature helps with a wide range of applications such as self-cleaning surfaces [10] and corrosion-proof metal surfaces [11]. Compared to anticorrosion in traditional protective coatings, superhydrophobic coating can be much efficient to reduce corrosion because it reduces the interaction between metal surface and corrosive species. To achieve that, several methods have been applied to produce a superhydrophobic surface such as wet chemical reaction [12], etching [13], and nanocomposite coating [14]. In nanocomposite coating, a bottom-up approach is used to grow a thin layer of well-chosen nanocomposite to create the superhydrophobization on the metal surface. The superhydrophobicity is created by the nanoparticles, while the polymer serves as a binder to connect the nanoparticles. When string bonding is achieved between polymer and nanoparticles, the mechanical properties of the coating will be enhanced [11]. Since polymers can be dissolved in a plenty of solvents, the spray deposition technique can be a suitable way to coat the metal where the solvent is evaporated rapidly after spraying and simply leaving a thin superhydrophobic coating on the surface of the metal. Therefore, spray method is appropriate for large-scale coating. The durability of nanocomposite superhydrophobic coatings is high, for instance, using SiO_2 nanoparticles with epoxy shows sustainability after 250min scouring test at 10m/s running water [15].

The anticorrosion mechanism of superhydrophobic coatings is described by formation of a thin air film between the liquid and the surface, which in turns reduces the contact area between them. This thin air film is called a nonconductive barrier and it is formed when air is trapped during immersion of the metal into the liquid. Therefore, the surface will be isolated from the surrounding liquid. Figure (2) illustrates the formation of the thin air film in the interface of a copper plate immersed in saline water [16]. The plate in the figure was half coated with superhydrophobic layer. As seen from the figure, the uncoated part is in intimate contact with the water with no interface barrier and it shows the red-orange color of the Cu plate, while the coated part forms a barrier of thin air that isolates the Cu surface from the saline water as it appears as a bubble-like region. This barrier reduces the contact area between the plate and water and hence, reduces the corrosion significantly.

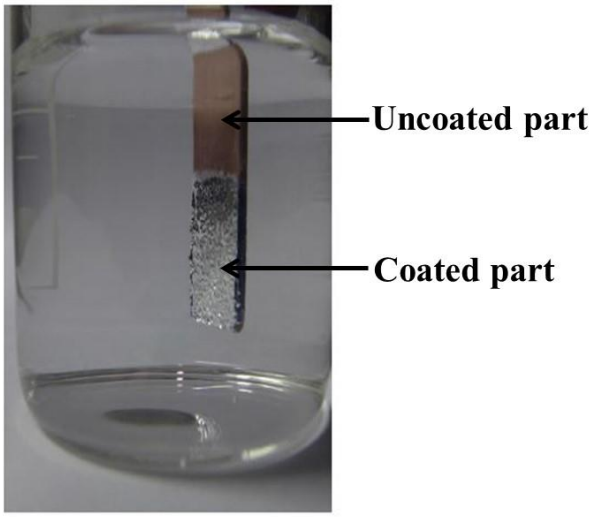

Figure 2 Cu plate immersed into 3.5 wt.% NaCl solution. *This figure is reproduced from* [16].

Despite that superhydrophobic nanocomposite applications have been widely investigated in the last recent years, the use of them as anticorrosion layer in low carbon steel is still immature with a little literature available [17,18]. The merit of this coating is that it is much more efficient than traditional anticorrosion coatings and it can be made as a very thin layer which makes it economically more viable. Thin layer is also more adhesive than thick layer with a less chance of peeling-off. This paper is an

attempt to study the anticorrosion resistance of low carbon steel (coated with manganese dioxide/polystyrene superhydrophobic nanocomposite) in aggressive media of acidic and saline solutions.

2. EXPERIMENTAL PROCEDURE

Manganese dioxide/polystyrene (MnO_2/PS) nanocomposites have been purchased from SAR Incorporation. The nanocomposite is comprised of MnO_2 nanoparticles in polystyrene matrix. The material was pre-dissolved in organic solvent and sold as a liquid-phase. The exact formula and synthesis recipe are the company know-how. The liquid-phase nanocomposite can be deposited by spray method. The deposited film has a free surface energy of ~13 mN/m and can achieve a contact angle of ~150° according to the company datasheet. These specifications represent superhydrophobicity features.
Low carbon steel (LCS) round samples of ~16 mm in diameter and 1 mm thick were used as a corrosion metal. The samples' chemical composition was determined using Optical Emission Spectrometer (OES) type ARL 3460. Table (1) shows the chemical composition of the used low carbon steel.

Table 1 Chemical composition of the used alloy.

Element	C	Si	S	P	Mn	Ni	Cr	Mo	Cu
Percent (%)	0.05	0.007	0.040	0.015	0.39	0.03	0.005	0.004	0.046

The samples were coated with the nanocomposite by spray method. Thickness of the coating was controlled by spraying time and estimated roughly using a gravimetric method. Five samples were prepared and marked as (S_1, S_2, S_3, S_4, and S_5) with approximate thickness of (21, 36, 77, 159, and 178 nm), respectively. Uncoated LCS was also used as a control sample and denoted as S_0. Figure (3) shows a photograph of the used samples after coating. Atomic Force Microscopy (AFM) type (Nanosurf FlexAFM) was used to probe the surface topography of the films.

Figure 3 The used samples after coating with MnO_2/PS nanocomposites.

Three-electrode potentiostat/galvanostat (Type M Lab) was used to carry out the electrochemical analysis. Saturated calomel was used as a reference electrode (the potential vs. the normal hydrogen electrode equals to +0.244V), graphite was served as a counter electrode, and the working electrode was the low carbon steel sample. Two corrosive solutions of 1M HCl and 5000ppm NaCl were used to investigate the corrosion. The exposed area of the samples was fixed at 0.79cm^2. Figure (4) shows a photograph of the experimental setup used in this work. Prior to the electrochemical measurements, the samples were kept in the solution for 15 min in order to stabilize the open circuit voltage. Polarization curves were recorded with a scan rate of 5mV/s. Samples were polarized according to the open circuit voltage (V_{OC}) of the sample, *i.e.* from $-V_{OC}$ to $+V_{OC}$. Corrosion current density (J) of the samples was calculated using Tafel method. The corrosion current density was obtained from dividing the measured current by the sample area. Using current density is important to normalize the results so that the

Exp. Theo. NANOTECHNOLOGY 5 (2021) 159 – 169

comparison between different samples is possible. The corrosion current was measured at various solution temperatures (20, 35, and 50°C) and from which, the activation energy (E_a) was calculated from Arrhenius equation [19]:

$$\log(I_{Corr}) = \log(A) - \frac{E_a}{2{,}303\ RT} \quad (1)$$

where: A is pre-exponential factor, R is the universal gas constant (8.314 J/K.mol), and T is the absolute temperature (in Kelvin). Corrosion protection efficiency (PE) was evaluated from [20]:

$$PE\ (\%) = \left[1 - \frac{I_{Corr}}{I^{o}_{Corr}}\right] \times 100\% \quad (2)$$

where: I^{o}_{Corr} and I_{Corr} are the corrosion currents of the superhydrophobic coated and uncoated LCS samples, respectively.

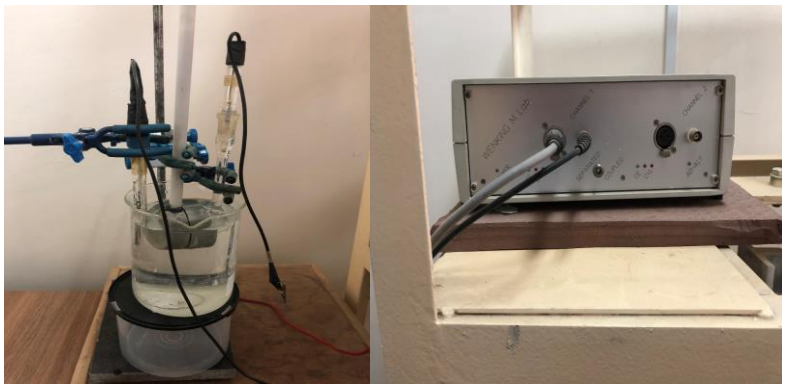

Figure 4 The experimental setup used in this work.

3. RESULTS AND DISCUSSION

Superhydrophobicity is a feature of the surface morphology rather than surface chemistry. It has been shown that a hierarchical structure can produce a superhydrophobic phenomenon [21]. This type of topography is characterized by the pyramid-like structure. Figure 5 shows a 3D AFM image of the MnO_2/PS nanocomposite film. The rms roughness is 109 nm which represents a very rough surface. The pinhole in the surface is due to a nonuniform deposition. The density of summit is low, but the summits are pyramid-like. Pinholes introduce corrosion sites and lessen the anticorrosion properties of the protective layer. To overcome this problem, different deposition methods such as printing method should be used in any future work.

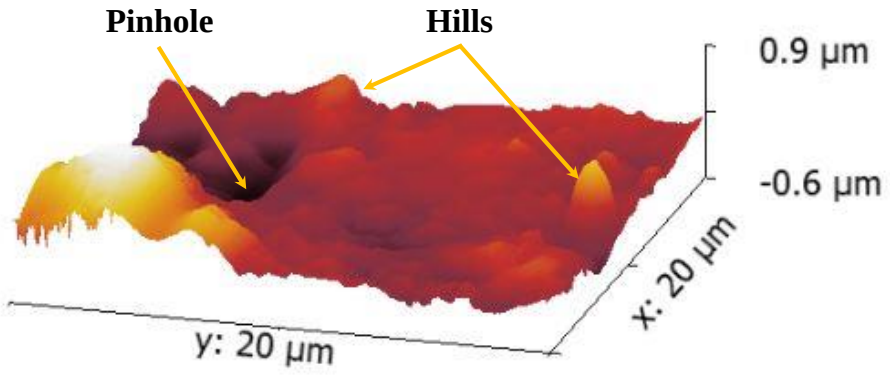

Exp. Theo. NANOTECHNOLOGY 5 (2021) 159 – 169

Figure 5 AFM image in a 3D mode for MnO_2/PS nanocomposite deposited on LCS surface.

Tafel method is used to determine the corrosion current density and the corrosion potential from the plot of the electrochemical redox process. The plot in Figure (6) shows two branches of reaction: anodic (in which a metal is oxidized), and cathodic (in which solution species are reduced). Absolute values of current density are plotted on a log-scale axis to undergo Tafel equation. Corrosion current density (J_{Corr}) and corrosion potential (E_{Corr}) are estimated from the intersection of the tangents of anodic and cathodic curves as demonstrated in this figure. The fitted tangents of all samples in this work were obtained with the aid of OriginLab software to perform best possible fitting with a statistical value of R-Squared of 0.99758. Fitting parameters are unified in all samples to cancel out any segment of error that may occur. The fitting lines were extrapolated so that they intersect, where intersection point represents J_{Corr} and E_{Corr} according to Tafel method as it is portrayed in the example of Figure (6).

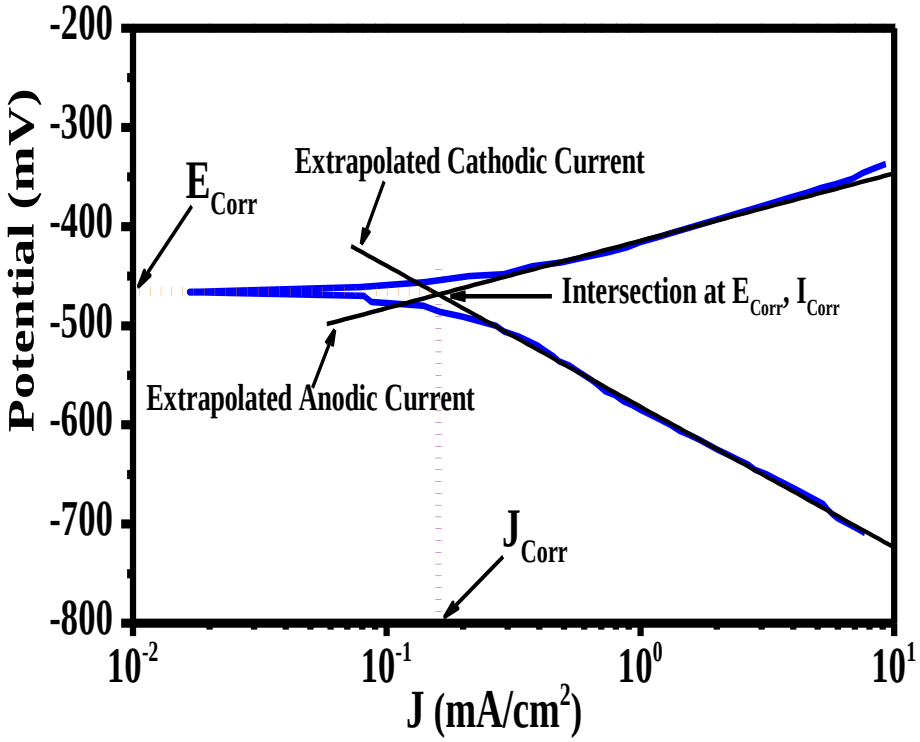

Figure 6 Tafel method used to determine corrosion parameters. The plot of this figure is for uncoated steel sample in 1M HCl solution.

Figure (7) illustrates potentiodynamic polarization curves in 1M HCl and 5000ppm NaCl aqueous solutions for S_0 and S_1 after 24 hours' immersion in the solutions. The J_{Corr} of S_0 and S_1 in HCl is 83.6 $\mu A/cm^2$ and 24.3 $\mu A/cm^2$, respectively. Whereas, J_{Corr} of S_0 and S_1 in NaCl is 14.4 $\mu A/cm^2$ and 0.56 $\mu A/cm^2$, respectively. The results show a significant decrease in corrosion current for the coated sample (S_1) compared with the uncoated control sample (S_0) in both solutions. Moreover, both coated and uncoated samples exhibit less corrosion current in NaCl solution than HCl solution. This is because LCS shows less corrosion in NaCl than HCl. Since HCl is a more aggressive solution, it may produce pinholes in the coated sample and penetrates into the LCS surface. However, the coating layer is still providing protection against the acid compared to the control sample.

Exp. Theo. NANOTECHNOLOGY 5 (2021) 159 – 169

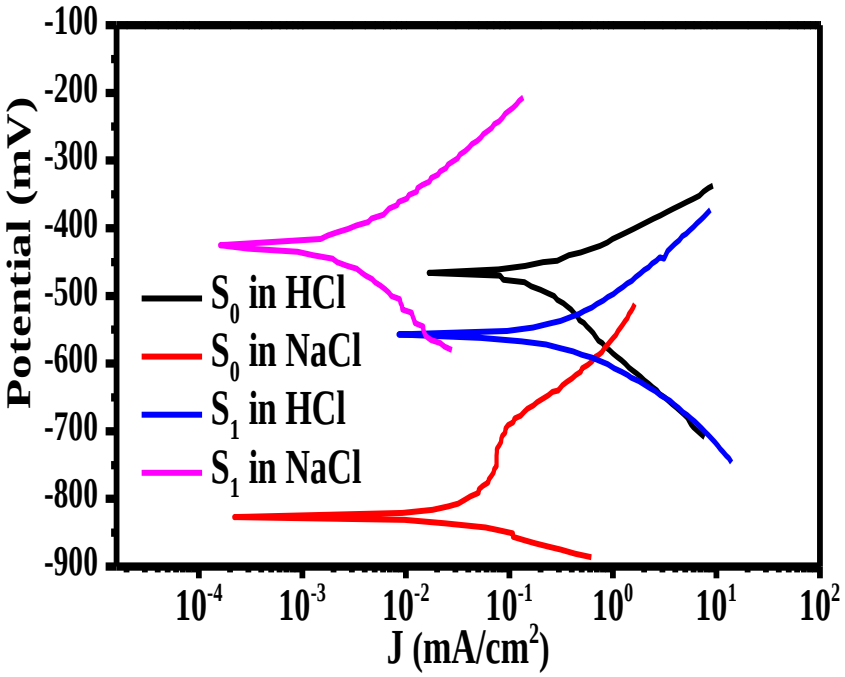

Figure 7 Potentiodynamic polarization curves in 1M HCl and 5000ppm NaCl for coated and uncoated samples.

Corrosion current density for uncoated sample and coated samples with different superhydrophobic layer thicknesses are presented in Figure (8). In the saline solution (NaCl), the corrosion current of S_1 sample exhibits a decrease around 25 folds in magnitude compared to the uncoated sample (S_0). Surprisingly, increasing thickness of the superhydrophobic layer results in an increase in the corrosion current. This indicates that in superhydrophobic coating, very thin layers provide better corrosion inhibition than thick layers. This can be attributed to the peeling effect for thicker layers. In addition, thick layers are less uniform and have more pinholes compared to thin layers. In the acidic solution (HCl), the corrosion current of S_1 sample exhibits a decrease around 3.5 folds in magnitude compared to the unprotected sample (S_0). This result shows that the MnO_2/PS superhydrophobic layer is less resistive in acidic media than saline media which driving this type toward the saline media applications rather than acidic media applications. The effect of thickness in the acidic solution is less than that of saline solution, where corrosion current shows a slight increase with increasing the coating layer.

Exp. Theo. NANOTECHNOLOGY 5 (2021) 159 – 169

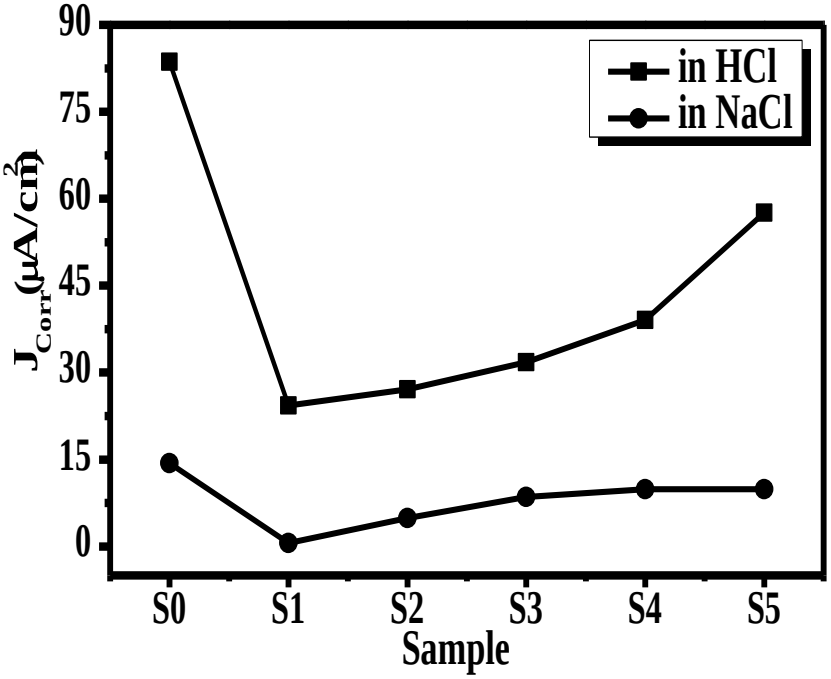

Figure (8) Corrosion current density for uncoated and coated samples with various thicknesses immersed in HCl and NaCl solutions for 24 hours.

Exposure time is a key factor in corrosion. To investigate the influence of immersion time on the evolution of corrosion current, the samples were immersed for one month in HCl and characterized every ten days, starting from 24 h immersion time. During the experiment, the samples kept in the solutions permanently for the whole month. The uncoated sample shows a sharp increase in corrosion current with time especially after 20 days. The coated sample shows an increase in corrosion with time, as well, but with a significantly less rate. The increased corrosion for the coated sample can be ascribed to the decrease in contact angle as acid removes some of the coated layer [17]. Decreasing contact angle results in wider contact between the acid and sample surface.

Exp. Theo. NANOTECHNOLOGY 5 (2021) 159 – 169

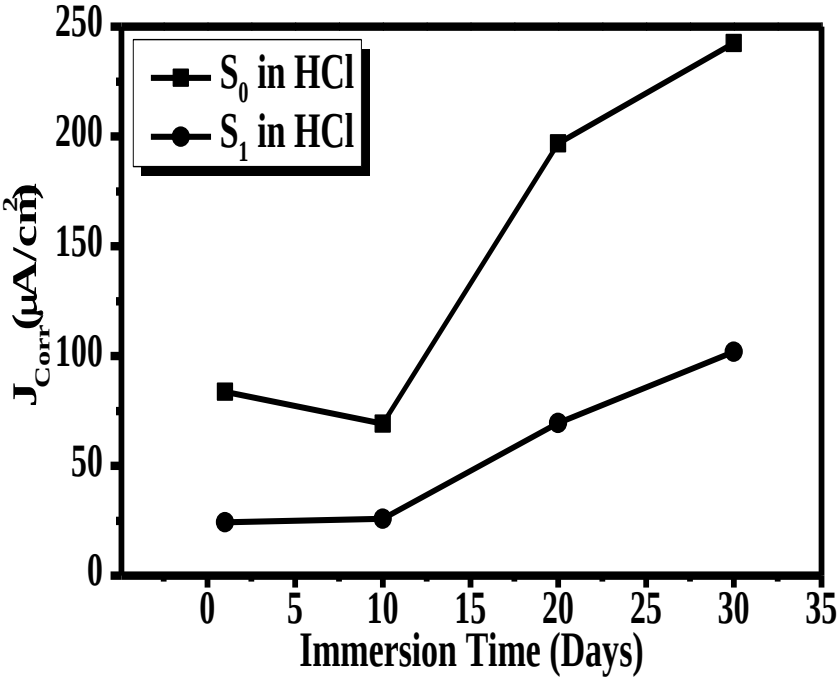

Figure 9 Corrosion current density for uncoated and coated samples with various immersion times in HCl solution.

Solution temperature impact on corrosion current for the samples in HCl solution is explored as shown in Figure (10-a). As solution temperature increases, the corrosion increases. This normal behavior can be exploited to determine activation energy of the surface as depicted in Figure (10-b) and described by Arrhenius [19] as shown earlier in Eq. (1). Activation energy of 34.7 kJ/mol and 47.3 kJ/mol for S_0 and S_1, respectively, are in fair agreement with literature for LCS [19]. The coated sample shows higher activation energy which is an indication of improving surface inhibition against corrosion.

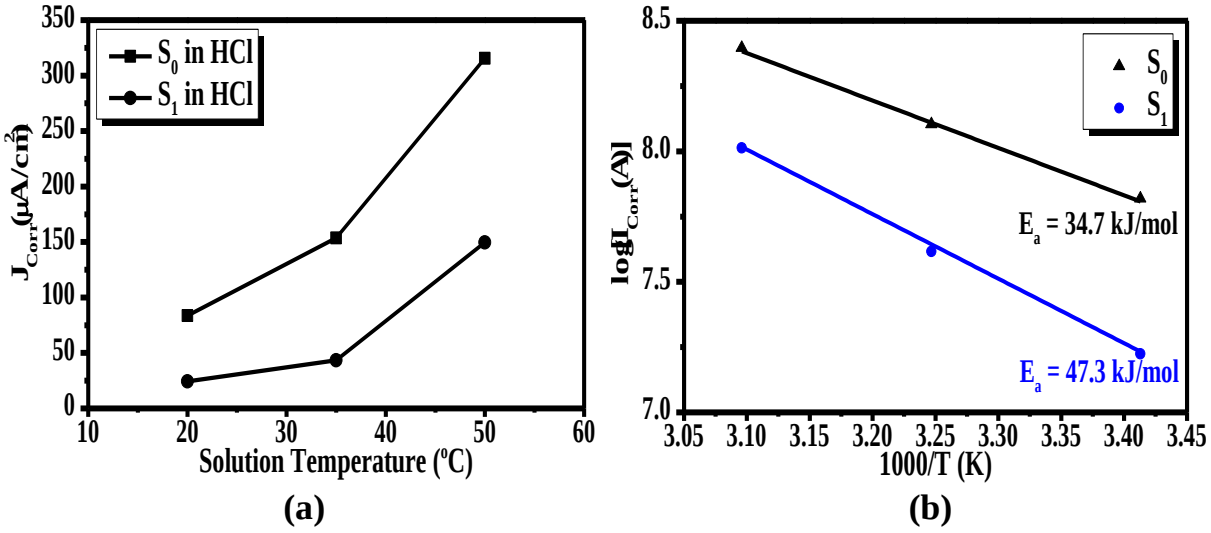

Figure (10) (a) Corrosion current density for uncoated and coated samples with various HCl solution temperatures, (b) Corrosion current density vs. the reciprocal of temperature.

Corrosion protection efficiency (PE) of the coated samples were calculated using Eq. (2) and presented in Figure (11). Lower thickness (S_1) shows better efficiency for both HCl and NaCl solutions, which can be attributed to the lower corrosion current for this sample as discussed in Figure (8) earlier. The efficiency decreases with increasing coating thickness which is consistent with the behavior of Figure (8). Highest efficiency recorded for S_1 sample at NaCl soltion with a value of 96.1%. However, steeper decrease in efficiency with coating thickness is observed in NaCl solution compared to HCl solution.
Pitting potential is determined in the forward scan. This is a destructive test for the coating, therefore, it was done at the last step of the measurement (after collecting the data of one month for the samples in HCl). The pitting potentials of S_0 and S_1 were 389 mV and 491 mV, respectively. The higher value of pitting potential for the coated sample indicates that the hydrophobic surface shows higher resistance against corrosion than the pristine sample.

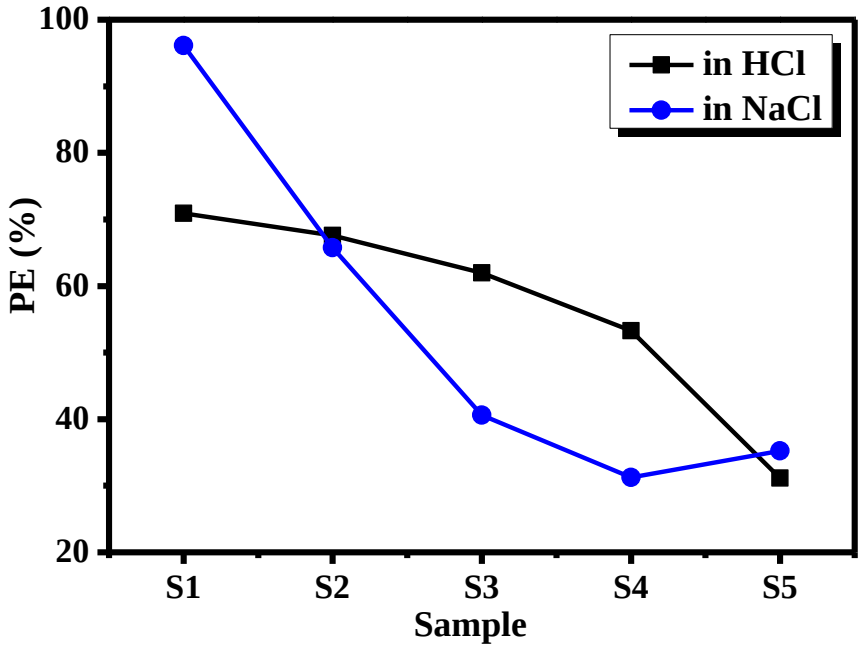

Figure (11) Protection efficiencies at various thicknesses of the coated samples.

4. CONCLUSIONS

Superhydrophobic surface comprised of MnO_2/PS nanocomposite layer can be used efficiently as anticorrosion coating in low carbon steel. The coating shows better inhibition in a saline medium (NaCl) than an acidic medium (HCl) with protection efficiency of up to 96.1% in NaCl solution. This result indicates that MnO_2/PS superhydrophobic nanocomposite layer is a candidate material for corrosion protection in the saline media. Various thicknesses of the nanocomposite were investigated in this work. Thickness showed a noticeable effect on the corrosion. Lower thickness has better inhibition than higher thickness. This is considered an economically viable result in the mass production industry.

5. ACKNOWLEDGEMENT

Financial and logistic support from the Renewable Energy and Environment Research Center and the Chemical and Petrochemical Research Center at the Corporation of Research and Industrial

Development are greatly appreciated. We would like to acknowledge the State Company for Steel Industries/ Ministry of Industry and Minerals for their assistance in the chemical analysis of the steel samples.

References

[1] Bassam Ramadhn Sarheed, Muhammed Abdul gafor, Mustafa. R. Al-Shaheen, Mohammed R. Alshaheen, Theo. Exp. NANOTECHOLOGY 4 (2020) 57
[2] R. Bhaskaran, N. Palaniswamy, N.S. Rengaswamy, M. Jayachandran, *Corros. Mater.* 13B (2005) 26
[3] K. Gerhardus, V. Jeff, N. Thopson, O. Moghissi, M. Gould, J. Payer, *International Measures of Prevention , Application , and Economics of Corrosion Technologies Study*, 2016.
[4] A. Stankiewicz, in: F. Pacheco-Torgal, M.V. Diamanti, A. Nazari, C.G. Granqvist, A. Pruna, S.B.T.-N. in E.C. (Second E. Amirkhanian (Eds.), *Woodhead Publ. Ser. Civ. Struct. Eng.*, Woodhead Publishing, (2019) 303
[5] C. de Souza, R.L.P. Teixeira, J.C. de Lacerda, C.R. Ferreira, C.H.B.S. Teixeira, V.T. Signoretti, *Polímeros* 28 (2018) 226
[6] R.-G. Hu, S. Zhang, J.-F. Bu, C.-J. Lin, G.-L. Song, *Prog. Org. Coatings* 73 (2012) 129.
[7] A. Marmur, *Langmuir* 20 (2004) 3517
[8] U. Cengiz, C. Elif Cansoy, *Appl. Surf. Sci.* 335 (2015) 99
[9] Y. Yu, Z.-H. Zhao, Q.-S. Zheng, Langmuir 23 (2007) 8212
[10] O.A. Abdulrazzaq, A. Abdullah, S.K. Abdulridha, M.A. Fakhri, *Iraqi J. Ind. Res.* 5 (2018) 1
[11] D. Zhang, L. Wang, H. Qian, X. Li, *J. Coatings Technol. Res.* 13 (2016) 11
[12] J. Song, Y. Lu, S. Huang, X. Liu, L. Wu, W. Xu, *Appl. Surf. Sci.* 266 (2013) 445
[13] D. Lv, J. Ou, M. Xue, F. Wang, *Appl. Surf. Sci.* 333 (2015) 163
[14] Y. Qing, C. Yang, C. Hu, Y. Zheng, C. Liu, *Appl. Surf. Sci.* 326 (2015) 48
[15] Z. Cui, L. Yin, Q. Wang, J. Ding, Q. Chen, *J. Colloid Interface Sci.* 337 (2009) 531
[16] P. Wang, D. Zhang, R. Qiu, Y. Wan, J. Wu, *Corros. Sci.* 80 (2014) 366
[17] L.B. Boinovich, S. V Gnedenkov, D.A. Alpysbaeva, V.S. Egorkin, A.M. Emelyanenko, S.L. Sinebryukhov, A.K. Zaretskaya, *Corros. Sci.* 55 (2012) 238
[18] A. Fihri, E. Bovero, A. Al-Shahrani, A. Al-Ghamdi, G. Alabedi, *Colloids Surfaces A Physicochem. Eng. Asp.* 520 (2017) 378
[19] A.A. Khadom, A.S. Yaro, A.S. Altaie, A.A.H. Kadum, *Port. Electrochim. Acta* 27 (2009) 699
[20] S. Habeeb, K. Saleh, in: IOP Conference Series: Materials Science and Engineering (Ed.), *IOP Conf. Ser. Mater. Sci. Eng.*, IOPscience, (2019) 96
[21] R. Wen, S. Xu, D. Zhao, Y.-C. Lee, X. Ma, R. Yang, *ACS Appl. Mater. Interfaces* 9 (2017) 44911

Exp. Theo. NANOTECHNOLOGY 5 (2021) 159 – 169